REPORT DOCUMENTATION PAGE

AFRL-SR-AR-TR-02-

0385

1. AGENCY USE ONLY *(Leave Blank)*	2. REPORT DATE	3. REPORT TYPE AND DATE COVERED
		Final Technical 010915-020930

3. TITLE AND SUBTITLE	5. FUNDING NUMBERS
Ultra-Wideband Antenna Development	C - F49620-01-C-0047
6. AUTHOR(S) John C. Riordan	
7. PERFORMING ORGANIZATION NAME(S) AND ADDRESS(ES) Titan Pulse Sciences Division P.O. Box 5010 San Leandro, CA 94577-0599	8. PERFORMING ORGANIZATION REPORT NUMBER 2119 JR
9. SPONSORING/MONITORING AGENCY NAMES(S) AND ADDRESS(ES) AF Office of Scientific Research 4015 Wilson Blvd. Mail Room 713 Arlington, VA 22203	10 SPONSORING/MONITORING AGENCY REPORT NUMBER

10. SUPPLEMENTARY NOTES

This work was sponsored by the Air Force Office of Scientific Research under appropriation number 57 13600 291 47B1 612304 6RNM25 59200 61002F 525700 F25700.

12a. DISTRIBUTUION AVAILABILITY STATEMENT	12b. DISTRIBUTION CODE
Approved for public release; distribution unlimited	

ABSTRACT (Maximum 200 words)

This report summarizes the results of a 1-year effort to investigate electromagnetic dispersion caused by finite electrical conductivity in ultra-wideband antennas. Integral equations are well-suited for antenna calculations, but numerical solutions of dispersive time-domain integral equations are extremely limited. The primary cause of this situation is the computational complexity, which increases by a factor or order N_t (the number of time steps) for dispersive materials. We propose an efficient solution based upon surface impedance boundary conditions and upon a recursive evaluation of the time convolution integral that has a complexity increase on the order of $\log(N_t)$. The numerical implementation of the efficient solution for a 2-dimensional planar transmission line is described in detail. Comparison of the efficient solution with the analytic solution of the same problem show good agreement in both time and frequency domains.

13. SUBJECT TERMS		15. PAGE COUNT
Computational electromagnetics Dispersive time-domain integral equation	Surface impedance boundary condition Recursive convolution Ultra-wideband antenna	32
		16. PRICE CODE

17. SECURITY CLASSIFICATION OF REPORT	18. SECURITY CLASSIFICATION OF THIS PAGE	19. SECURITY CLASSIFICATION OF ABSTRACT	20. LIMITATION OF ABSTRACT
UNCLASSIFIED	UNCLASSIFIED	UNCLASSIFIED	

1122 135

Ultra-Wideband Antenna Development Final Technical Report

September 2002

AFOSR Contract Number F949620-01-C-0047

Submitted To
Dr. Arje Nachman
Mathematics and Space Sciences Directorate
Air Force Office of Scientific Research

Prepared by
Dr. John C. Riordan
Pulse Sciences Division
Titan Systems Corporation

TITAN SYSTEMS CORPORATION
PULSE SCIENCES DIVISION
2700 Merced Street, San Leandro, CA 94577-0599
Telephone: (510) 357-4610 • Fax: (510) 577-7247 • http://www.titan.com

Table of Contents

SECTION 1

SUMMARY

Unlike a conventional radar signal, an ultra-wideband (UWB) radar signal contains a wide spectrum of frequency components that are subject to dispersive effects. The radiated and received signal shapes will be altered not only by frequency-dependent losses in the antenna conductors, but also by wavelength-dependent reflections from geometry transitions in the antenna. These antenna-dependent effects must be minimized and characterized before a meaningful target analysis can be performed. The antenna effects can in principle be treated computationally using time-domain integral equations, which offer several advantages over alternative approaches using either the frequency domain or finite differences.

The solution of dispersive time-domain integral equations for practical three-dimensional problems has been severely limited by the additional computational complexity, which typically increases by a factor of N_t (number of time steps) over the corresponding ideal problem with perfect electrical conductors. The primary result of our work is the development of an efficient solution whose computational complexity increases by a factor of only $\log(N_t)$ over the corresponding ideal problem. This efficient solution will facilitate the use computational techniques for the design of UWB antennas and for the analysis of transmitted and received signals.

Section 2 summarizes dispersive effects in metal conductors. We conclude that the conventional low-frequency model for electrical conductivity is an excellent approximation for frequencies of interest for UWB radar, and that there is no experimental or theoretical evidence of other effects that need to be included until the frequency exceeds 100 GHz.

Section 3 summarizes the existing treatment of time-domain integral equations for three-dimensional electromagnetics. Most of this work treats non-dispersive problems, i.e., perfect electrical conductors or perfect dielectrics. Although time-domain integral equations have been formulated for dispersive media, i.e., lossy conductors or dielectrics, only limited solutions for simple geometry have been achieved because of the computational challenges.

In Section 4 we present an efficient method for the solution of dispersive time-domain integral equations in three dimensions. We use surface impedance boundary conditions to avoid any increase in the number of scalar integral equations that need to be solved. The resulting equations still contain additional time-convolution integrals that increase computational time requirements by a factor of N_t. However, we have developed a simple recursion relation for the convolution so that the computational complexity only increases by a factor of order $\log(N_t)$ over the corresponding ideal problem.

In Section 5 we describe in detail the numerical implementation of the efficient solution for a two-dimensional problem involving a lossy planar transmission line. We determine the incident fields for a wave that is fed at the center of the line, and then reduce the time and space

integrals to summations that can be performed numerically. The resulting equations are then solved numerically by time-stepping as for the ideal time-domain integral equation..

In Section 6 we validate our approach by comparing the computational and analytical solutions for the two-dimensional planar transmission line, both lossy and ideal. We find good agreement between the computational and analytic results in both the time and frequency domains.

Sections 7 and 8 contain code listings and references, respectively.

SECTION 2

ELECTROMAGNETIC DISPERSION IN METALS

Soon after the discovery of the electron, Drude [1] proposed a theory of electrical conductivity based upon the assumption that there is a gas of free electrons in a metal. Electrical resistance arises from the collisions of accelerated electrons with the background atoms. Drude's phenomenological theory gives an expression for the low-frequency conductivity

$$\sigma_0 = \frac{ne^2}{m\gamma} = \frac{\varepsilon_0 \omega_p^2}{\gamma},$$

where e and m are the charge and mass of the electron, n is the electron density, γ is the collision rate, ε_0 is the vacuum permittivity, and ω_p is the electron plasma frequency given by

$$\omega_p^2 = \frac{ne^2}{\varepsilon_0 m}.$$

Modern theories of electrical conductivity (Bardeen [2] and Kittel [3]) show that that the electron collisions are dominated by scattering from thermal vibrations of the metal atom lattice rather than from individual metal atoms, but the above phenomenological expression remains valid.

At higher frequency one must include electron inertia as well as collisions. The phenomenological equation for the electron velocity then becomes

$$m\dot{v} + mv\gamma = eE\exp(-i\omega t).$$

Then one obtains a complex conductivity

$$\sigma = \frac{ne^2}{m(\gamma - i\omega)} = \frac{\varepsilon_0 \omega_p^2}{(\gamma - i\omega)},$$

and a corresponding dielectric function

$$\varepsilon(\omega) = \varepsilon_0 - \frac{\sigma}{i\omega} = \varepsilon_0\left(1 - \frac{\omega_p^2}{\omega(\omega + i\gamma)}\right).$$

This dielectric is a function of frequency and thus causes dispersion in wave propagation. We have searched the literature extensively, but have not found any theoretical or experimental basis for other effects that should be included in a high-frequency conductivity model for metals.

A comparison of key conductivity parameters for three common metals, copper (commercial annealed), aluminum (type 6061-T6), and stainless steel (type 304) is presented in Table 2.1. One would expect high-frequency conductivity effects to become significant at frequencies comparable to the collision frequency, which is about 10^{13} Hz (far infra-red). Indeed, Stratton [4] quotes experimental data showing that the low-frequency conductivity is valid up to about

10^{13} Hz. This frequency is a factor of more than 100 higher than the tens of GHz that is envisioned for UWB radar. For frequencies above the plasma frequency at about 3×10^{15} Hz (ultraviolet), the dielectric has a positive real component and waves will propagate rather than attenuate. Kittel [3] presents experimental data that confirm the ultraviolet transmission window for thin metal films.

Table 2-1. High-frequency conductivity parameters for common metals.

Metal	Low-frequency conductivity σ_0 (mho/m)	Conduction electron density (m^{-3})	Collision frequency $\gamma/2\pi$ (Hz)	Plasma frequency $\omega_p/2\pi$ (Hz)
Copper (comm. anld.)	5.80×10^7	8.45×10^{28}	6.53×10^{12}	2.61×10^{15}
Aluminum (6061-T6)	2.50×10^7	1.81×10^{29}	3.24×10^{13}	3.82×10^{15}
Stainless steel (304)	1.40×10^6	1.70×10^{29}	5.44×10^{14}	3.70×10^{15}

Thus, the simpler low-frequency conductivity model is valid for metals and frequencies of interest for UWB radar. In the remainder of this report we will assume that the metals are good but nevertheless lossy conductors. Physically, this means $\omega << \gamma << \omega_p$, so that the complex dielectric function is well-approximated by

$$\varepsilon(\omega) = \varepsilon_0(1 - \sigma / i\omega\varepsilon_0), \quad \sigma / \omega\varepsilon_0 >> 1.$$

We will also suppress the zero subscript, so that σ will always represent the low-frequency (or "dc") conductivity.

SECTION 3

TIME-DOMAIN INTEGRAL EQUATIONS

In 1968 Bennet and Weeks [5,6] introduced a novel approach for solving the time-domain integral equation for the scattering of electromagnetic waves from perfectly conducting, two- and three-dimensional bodies. Instead of resorting to the matrix solution typical of frequency-domain solutions, they used a time-stepping approach similar to that used for solving initial value problems. Early reviews by Poggio and Miller [7] and Mittra [8] provide detailed derivations of the basic equations and extensive details of the computational implementations. A more recent review by Miller [9] summarizes applications of the time-domain approach, all of which are limited to perfect conductors. Although Tesche [10] investigated the time-domain integral equation for lossy conductors in 1991, the first numerically rigorous solution for a three-dimensional problem was reported ten years later by Bluck et al [11].

We first review the three-dimensional time-domain integral equations for propagation in a linear, isotropic, homogeneous medium. Poggio and Miller [7, equ. 4.35 & 4.37] give the electric and magnetic field integral equations (EFIE and MFIE respectively) for a source-free volume bounded by a closed surface S (part of which may be at infinity)

$$\frac{\Omega}{4\pi}\mathbf{E} = \mathbf{E}^{inc} - \frac{1}{4\pi}\oint_S ds' \int dt' \frac{\delta(t'-t+R/c)}{R}\left\{\mu\frac{\partial}{\partial t'}[\mathbf{n}'\times\mathbf{H}'] - \left[\frac{1}{R}+\frac{1}{c}\frac{\partial}{\partial t'}\right][[\mathbf{n}'\times\mathbf{E}']\times\hat{\mathbf{R}} + [\mathbf{n}'\cdot\mathbf{E}']\hat{\mathbf{R}}]\right\}$$

$$\frac{\Omega}{4\pi}\mathbf{H} = \mathbf{H}^{inc} + \frac{1}{4\pi}\oint_S ds' \int dt' \frac{\delta(t'-t+R/c)}{R}\left\{\varepsilon\frac{\partial}{\partial t'}[\mathbf{n}'\times\mathbf{E}'] + \left[\frac{1}{R}+\frac{1}{c}\frac{\partial}{\partial t'}\right][[\mathbf{n}'\times\mathbf{H}']\times\hat{\mathbf{R}} + [\mathbf{n}'\cdot\mathbf{H}']\hat{\mathbf{R}}]\right\}$$

Here bold type denotes vector quantities, and

$\mathbf{E} = \mathbf{E}(\mathbf{r},t)$ is the electric field at the observation point;
$\mathbf{E}' = \mathbf{E}(\mathbf{r}',t')$ is the electric field at the source point on the surface S;
$\mathbf{E}^{inc} = \mathbf{E}^{inc}(\mathbf{r},t)$ is the incident electric field generated by sources outside of S, typically a plane wave from infinity or a current at an antenna feed;
Similar conventions hold for $\mathbf{H}$, $\mathbf{H}'$, and $\mathbf{H}^{inc}$;
$\Omega = \Omega(\mathbf{r})$ is the solid angle subtended by the medium at the observation point, e.g. 2π on a smooth surface S or 4π in the enclosed volume;
δ is the Dirac delta function;
ε and μ are the electric permittivity and magnetic permeability, respectively;
$c = (\varepsilon\mu)^{-0.5}$ is the speed of light in the medium;
$\mathbf{R} = \mathbf{r} - \mathbf{r}'$, $R = |\mathbf{R}|$, and $\hat{\mathbf{R}}$ is the unit vector;
$\mathbf{n}'$ is a unit normal to S pointing into the enclosed volume;
$\oint_S$ is a principal value integral on the surface S.

Note that the time integral is trivial for non-dispersive media, with the source quantities simply evaluated at the retarded time $t' = t - R/c$.

When the surface S coincides with a perfect electrical conductor (PEC), the electric and magnetic fields must satisfy boundary conditions given by

$$\mathbf{n}\times\mathbf{E}(\mathbf{r},t)=0 \quad \text{and} \quad \mathbf{n}\cdot\mathbf{H}(\mathbf{r},t)=0\,.$$

For perfect electrical conductors it is also useful to define the surface current and charge density

$$\mathbf{J}_S(\mathbf{r},t)=\mathbf{n}\times\mathbf{H}(\mathbf{r},t)$$

$$\rho_S(\mathbf{r},t)=\varepsilon\mathbf{n}\cdot\mathbf{E}(\mathbf{r},t)\,,$$

which satisfy a conservation relation

$$\frac{\partial}{\partial t}\rho_S(\mathbf{r},t)+\nabla\cdot\mathbf{J}_S(\mathbf{r},t)=0\,.$$

Taking the cross-product with the normal $\mathbf{n}$ to the surface S, and using $\Omega=2\pi$ for $\mathbf{r}$ on S, the EFIE and MFIE can then be written as

$$\mathbf{n}\times\mathbf{E}^{inc}(\mathbf{r},t)=\frac{1}{4\pi}\oint_S ds'\left\{\frac{\mu}{R}\frac{\partial}{\partial t'}\mathbf{J}_S(\mathbf{r}',t')-\left[\frac{1}{R^2}+\frac{1}{Rc}\frac{\partial}{\partial t'}\right]\frac{\rho_S(\mathbf{r}',t')}{\varepsilon}\right\}_{t'=t-R/c}$$

$$\mathbf{J}_S(\mathbf{r},t)=2\mathbf{n}\times\mathbf{H}^{inc}(\mathbf{r},t)+\frac{\mathbf{n}}{2\pi}\times\oint_S ds'\left\{\left[\frac{1}{R^2}+\frac{1}{Rc}\frac{\partial}{\partial t'}\right]\mathbf{J}_S(\mathbf{r}',t')\times\hat{\mathbf{R}}\right\}_{t'=t-R/c}.$$

Either one of these equations suffices to determine the two scalar components of $\mathbf{J}_S$, which in turn determines the electric and magnetic fields in the volume enclosed by S. Miller notes that the MFIE is best suited for smooth closed conductors, while the EFIE is applicable to more general bodies including thin wires and shells.

When the surface S coincides with a lossy conductor, then one must solve a second pair of integral equations for the lossy medium, and then match boundary conditions across S. Bluck et al [11] write the EFIE and MFIE for a lossy conductor (using the same convention for observation and source points) as

$$\frac{\Omega}{4\pi}\mathbf{E}=\frac{1}{4\pi}\oint_S ds'\int dt'\left\{\left[\mu\mathbf{n}'\times\frac{\partial\mathbf{H}'}{\partial t'}\right]G-(\mathbf{n}'\times\mathbf{E}')\times\nabla'G-(\mathbf{n}'\cdot\mathbf{E}'')\times\nabla'G\right\}$$

$$\frac{\Omega}{4\pi}\mathbf{H}=\frac{1}{4\pi}\oint_S ds'\int dt'\left\{-\left[\sigma\,\mathbf{n}'\times\mathbf{E}'+\varepsilon\mathbf{n}\times\frac{\partial\mathbf{E}'}{\partial t'}\right]G-(\mathbf{n}'\times\mathbf{H}')\times\nabla'G-(\mathbf{n}'\cdot\mathbf{H}')\times\nabla'G\right\},$$

$$G(r,t;r',t')=\exp(-\beta\tau)\left[\frac{\delta(\tau-R/c)}{R}+\frac{\beta/c}{\sqrt{\tau^2-R^2/c^2}}I_1(\beta\sqrt{\tau^2-R^2/c^2})\,\theta(\tau-R/c)\right].$$

Here G(r,t;r',t') is the Green's function given by Morse and Feshbach [12], the material properties now refer to the lossy medium, and

$\beta=\sigma/2\varepsilon$ is the characteristic decay rate;
$\mathbf{n}'$ is a unit surface normal directed away from the lossy body;
$\tau=t-t'$;

I_1 is the first-order modified Bessel function of the first kind;
θ is the Heaviside unit step function.

The boundary conditions at the interface S between the ideal dielectric (subscript 1) and the lossy conductor (subscript 2) are given by

$$\varepsilon_1 \, \mathbf{n} \cdot \mathbf{E}_1(t) = \varepsilon_2 \, \mathbf{n} \cdot \mathbf{E}_2(t) + \sigma_2 \int_0^t du \; \mathbf{n} \cdot \mathbf{E}_2(u)$$

$$\mathbf{n} \cdot (\mathbf{B}_1 - \mathbf{B}_2) = 0$$

$$\mathbf{n} \times (\mathbf{E}_1 - \mathbf{E}_2) = 0$$

$$\mathbf{n} \times (\mathbf{H}_1 - \mathbf{H}_2) = 0 \, .$$

Bluck et al [11] have computed the scattering of a gaussian plane wave by a lossy dielectric sphere, and have obtained good agreement with the analytical solution

Nevertheless, the computational complexity of the lossy time-domain integral equation has prevented its application to practical problems. This complexity arises primarily for three reasons. First of all, the lossy problem requires a true time integration (rather than a delta-function) at each space point for each time step, which increases the computational complexity by a factor of order N_t, the number of time steps. Second, the lossy problem requires the computation of 12 field components (3 electric and 3 magnetic for both media) at each point in space and time, compared to only two components of $\mathbf{J}_S$ for the PEC problem. Finally, the lossy Green's function requires the evaluation of exponential and Bessel functions, rather than the simpler 1/R of the PEC problem. In the following section we propose an alternative approach that greatly mitigates the complexity introduced for the first two reasons.

SECTION 4

EFFICIENT SOLUTION FOR LOSSY CONDUCTORS

In this section we propose an efficient solution for the dispersive time-domain integral equation that applies when the conductivity is high enough that the electromagnetic skin depth is much smaller than any geometric scale length. For small skin depth the problem can be greatly simplified by the use of an impedance boundary condition at the surface of the material. We then use an improved exponential approximation for the surface impedance and develop a recursion relation that greatly reduces the computation involved in performing the convolution integral.

The surface impedance boundary condition (SIBC) is attributed to Leontovich [13], but Senior [14] provides a more accessible exposition. Mitzner [15] first used the SIBC in a frequency-domain integral equation approach to scattering from a body of finite conductivity. Tesche [10] first applied the SIBC to a time-domain integral equation, but his non-rigorous approach resulted in errors that we have corrected below.

We assume the conductor is a good conductor, i.e., $\sigma >> \omega\varepsilon$ for all frequencies of interest, and that the skin depth

$$\delta = \sqrt{\frac{2}{\mu\omega\sigma}}$$

is negligible compared to the wavelengths of interest, to the radii of curvature, and to any other geometric scale lengths in the problem. We have rewritten Senior's [14] frequency-domain SIBC in terms of a normalized impedance Z that is a function of the Laplace variable s,

$$\mathbf{E} - (\mathbf{n}\cdot\mathbf{E})\mathbf{n} = \sqrt{\frac{\mu_c}{\varepsilon_c}}\, Z\, \mathbf{n}\times\mathbf{H}$$

$$Z \equiv \sqrt{\frac{s}{s+2\beta}}, \quad \beta \equiv \frac{\sigma_c}{2\varepsilon_c}.$$

Here $\mathbf{n}$ is the unit surface normal pointing away from the conductor, and the subscript c refers to conductor properties. Taking the cross-product with $\mathbf{n}$, the SIBC can be rewritten as a surface Ohm's law

$$\mathbf{n}\times\mathbf{E} = \sqrt{\frac{\mu_c}{\varepsilon_c}}\, Z\, \mathbf{J}_S.$$

To obtain a boundary condition for the normal component of the magnetic field we rewrite Senior's result using the normal derivative of $\mathbf{H}$ as

$$\mathbf{n}\cdot\mathbf{H} = c\sqrt{\frac{\mu_c}{\varepsilon_c}\frac{\varepsilon}{\mu}}\, Y\, \mathbf{n}\cdot(\mathbf{n}\cdot\nabla\mathbf{H})$$

$$Y = \sqrt{\frac{1}{s(s+2\beta)}}, \quad \beta = \frac{\sigma_c}{2\varepsilon_c},$$

where Y is a normalized pseudo-impedance. We then use $\nabla \cdot \mathbf{H} = 0$ and $\nabla \cdot \mathbf{n} = \nabla \mathbf{n} = 0$ for Cartesian coordinates to express the normal derivative in terms of the surface current

$$\nabla \times (\mathbf{n} \times \mathbf{H}) = \mathbf{H} \cdot \nabla \mathbf{n} - \mathbf{n} \cdot \nabla \mathbf{H} + \mathbf{n} \nabla \cdot \mathbf{H} - \mathbf{H} \nabla \cdot \mathbf{n} = -\mathbf{n} \cdot \nabla \mathbf{H}.$$

Thus, we obtain desired boundary condition on the normal component of H,

$$\mathbf{n} \cdot \mathbf{H} = -c \sqrt{\frac{\mu_c}{\varepsilon_c} \frac{\varepsilon}{\mu}}\, Y\, \mathbf{n} \cdot \nabla \times \mathbf{J}_s.$$

Since the above SIBCs on $\mathbf{n} \times \mathbf{E}$ and $\mathbf{n} \cdot \mathbf{H}$ are in the frequency domain, we must perform the inverse Laplace transforms to obtain the corresponding boundary conditions in the time domain. Using standard Laplace transform tables we obtain

$$Z(t) = \delta(t) - \beta\, e^{-\beta t}\, [I_0(\beta t) - I_0(\beta t)] \equiv \delta(t) - \beta Z_1(t)$$

$$Y(t) = e^{-\beta t}\, I_0(\beta t),$$

where I_0 and I_1 are modified Bessel functions of the first kind. The time-domain boundary conditions then involve convolution integrals

$$\mathbf{n} \times \mathbf{E} = \sqrt{\frac{\mu_c}{\varepsilon_c}}\, Z * \mathbf{J}_S$$

$$\mathbf{n} \cdot \mathbf{H} = -c \sqrt{\frac{\mu_c}{\varepsilon_c} \frac{\varepsilon}{\mu}}\, Y * \mathbf{n} \cdot \nabla \times \mathbf{J}_s$$

$$\text{where} \quad f * g \equiv \int_0^t dt\, f(u)\, g(t-u).$$

In the limit of perfect conductivity ($\beta \to \infty$) these boundary conditions reduce to those for a PEC, i.e., $\mathbf{n} \times \mathbf{E} = \mathbf{n} \cdot \mathbf{H} = 0$.

To obtain the time-domain integral equations for a region bounded by a lossy conductor, we first take the cross-product with $\mathbf{n}$ of the first EFIE and MFIE of the preceding section, giving

$$\frac{\Omega}{4\pi} \mathbf{n} \times \mathbf{E} = \mathbf{n} \times \mathbf{E}^{inc} - \frac{\mathbf{n}}{4\pi} \times \oint_S ds' \frac{1}{R} \left\{ \mu \frac{\partial}{\partial t'} [\mathbf{n}' \times \mathbf{H}'] - \left[\frac{1}{R} + \frac{1}{c} \frac{\partial}{\partial t'} \right] [[\mathbf{n}' \times \mathbf{E}'] \times \hat{\mathbf{R}} + [\mathbf{n}' \cdot \mathbf{E}'] \hat{\mathbf{R}}] \right\}_{t'=t-R/c}$$

$$\frac{\Omega}{4\pi} \mathbf{n} \times \mathbf{H} = \mathbf{n} \times \mathbf{H}^{inc} + \frac{\mathbf{n}}{4\pi} \times \oint_S ds' \frac{1}{R} \left\{ \varepsilon \frac{\partial}{\partial t'} [\mathbf{n}' \times \mathbf{E}'] + \left[\frac{1}{R} + \frac{1}{c} \frac{\partial}{\partial t'} \right] [[\mathbf{n}' \times \mathbf{H}'] \times \hat{\mathbf{R}} + [\mathbf{n}' \cdot \mathbf{H}'] \hat{\mathbf{R}}] \right\}_{t'=t-R/c}$$

Next we insert the above time-domain boundary conditions and use the charge conservation relation between $\mathbf{J}_S$ and ρ_S to obtain

$$\frac{\Omega}{4\pi} Z * \mathbf{J}_S = \mathbf{n} \times \mathbf{E}^{inc} - \frac{\mathbf{n}}{4\pi} \times \oint_S ds' \frac{1}{R} \left\{ \mu \frac{\partial}{\partial t'} \mathbf{J}'_S - \left[\frac{1}{R} + \frac{1}{c} \frac{\partial}{\partial t'} \right] \left[Z' * \mathbf{J}'_S \times \hat{\mathbf{R}} + \frac{\hat{\mathbf{R}}}{\varepsilon} \nabla' \cdot \int_0^{t'} du\, \mathbf{J}'_S(u) \right] \right\}_{t'=t-R/c}$$

$$\frac{\Omega}{4\pi} \mathbf{J}_S = \mathbf{n} \times \mathbf{H}^{inc} + \frac{\mathbf{n}}{4\pi} \times \oint_S ds' \frac{1}{R} \left\{ \mathbf{n}' \times \frac{\partial}{c\partial t'} Z' * \mathbf{J}'_S + \left[\frac{1}{R} + \frac{1}{c} \frac{\partial}{\partial t'} \right] \left[\mathbf{J}'_S \times \hat{\mathbf{R}} + \mathbf{n}' \cdot \nabla' \times (Y' * \mathbf{J}'_S) \hat{\mathbf{R}} \right] \right\}_{t'=t-R/c}$$

Since either equation suffices to determine the surface current density $\mathbf{J}_S$, we have reduced the number of scalar field quantities from twelve to two. Thus, we have eliminated the second complexity issue raised at the end of the preceding section. Furthermore, we have corrected the error in Tesche's result, which omitted the convolution $Z' * \mathbf{J}'_S$ term for source points on S.

These integral equations still involve a true time integration in the convolution term. The computational complexity can be greatly reduced if the convolution integral can be recursively updated. In 1990 Luebbers et al [16] demonstrated that a recursive convolution was possible for a time-domain dielectric susceptibility given by a simple exponential function. The recursive convolution integral was soon applied to a finite-difference time-domain SIBC by Maloney and Smith [17], who used Prony's method to approximate the surface impedance by a sum of exponentials. Oh and Schutt-Aine [18] fitted a minimax rational approximation to the frequency-domain impedance, then decomposed the fit into a sum of simple poles and obtained an exponential sum representation for the surface impedance in the time domain. Unfortunately, Prony's method requires a large number of exponential terms for a good approximation over a large number of time steps, while Oh's approach gives a poor approximation in the time domain. These problems arise primarily from the huge variation in the time domain impedance $Z_I(u)$, which asymptotically approaches $u^{-3/2}$ for large arguments u.

To obtain an improved exponential-sum approximation using a limited number of terms, we have used a different approach to determine the exponents and coefficients in the fit

$$Z_I(\beta t) = \sum_{m=1}^{M} c_m \exp(-\omega_m \beta t).$$

Specifically, we have chosen the exponents ω_i to span the range $[(3N_t\beta\Delta)^{-1}, 3\beta\Delta]$ in a logarithmically uniform manner, where Δ is the time step and N_t is the number of steps in the numerical implementation. Then the coefficients c_i are determined by a least squares fit to $Z_I(n\beta\Delta)$ over the range $1 \le n \le N_t$, again using logarithmically uniform spacing for n. As shown in Figure 4-1, this approach provides an excellent minimax approximation to Z_I over the entire time range for the computation. The number of terms required depends upon the desired relative error ($\delta Z/Z$) as well as the number of time steps, and is approximately given by

$$M \approx 2 \log_{10}\left(N_t \frac{Z}{\delta Z} \right);$$

M = 10 terms give a relative error of <0.2% over 10^3 time steps.

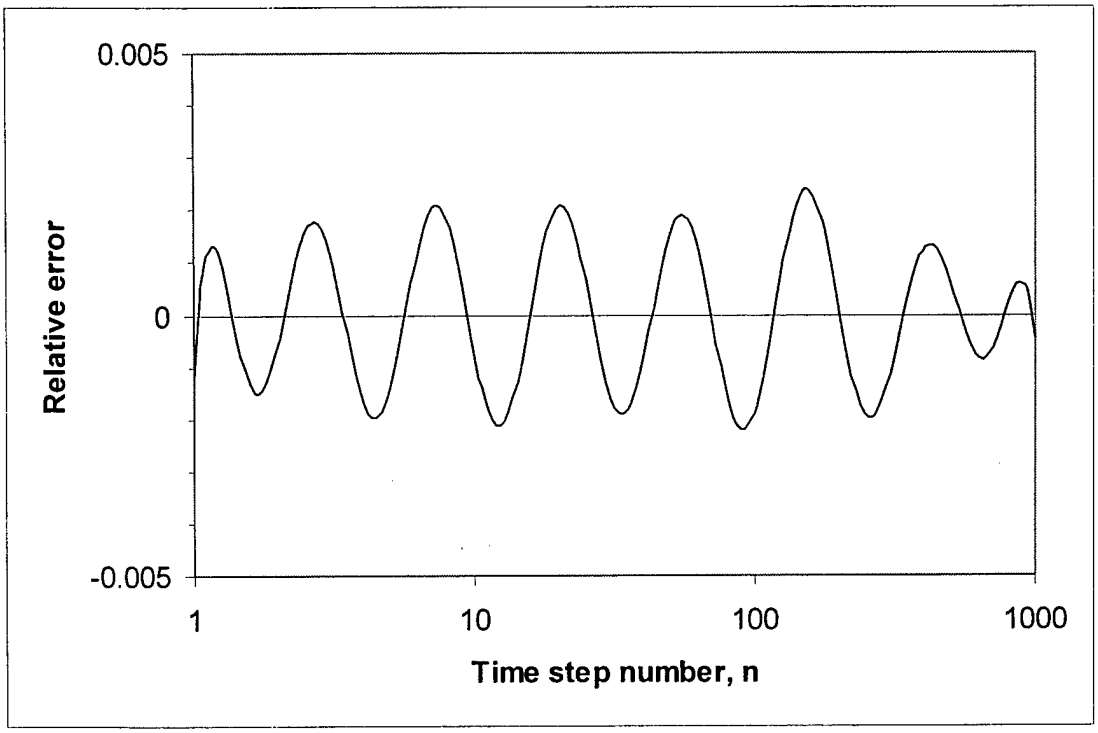

Figure 4-1. Relative error for a 10-term exponential fit to the normalized impedance $Z_1(n\beta\Delta)$.

Before using the exponential fit in the convolution integral, we have found it helpful to separate out the time interval $[0,\Delta]$ and to rewrite the scalar convolution integral as the sum (suppressing the spatial argument for simplicity)

$$
\begin{aligned}
E(t) \equiv Z * J &= \int_0^{t-\Delta} du\, Z(t-u)\, J(u) + \int_{t-\Delta}^{t} du\, Z(t-u)\, J(u) \\
&= \int_{t-\Delta}^{t} du\, Z(t-u)\, J(u) - \int_0^{t-\Delta} du\, \beta\, Z_1(\beta(t-u))\, J(u) \\
&= \int_0^{\Delta} dv\, [\delta(v) - \beta\, Z_1(\beta t)]\, J(t-v) - \sum_{m=1}^{M} c_m \int_0^{t-\Delta} du\, \beta \exp(-\omega_m \beta(t-u))\, J(u) \\
&\equiv E_0(t) - \sum_{m=1}^{M} E_m(t) \quad .
\end{aligned}
$$

Assuming that the time step Δ is chosen small enough that J(t) is nearly constant, we can pull J(t) outside the $E_0(t)$ integral and use [19, equ. 6.611.4]

$$\int_0^{\infty} du\, Z_1(u) = 1$$

to obtain an accurate small difference between two large terms

$$E_0(t) = J(t) - J(t) \int_0^{\beta\Delta} dv\, Z_1(v) = J(t) \int_{\beta\Delta}^{\infty} dv\, Z_1(v) \quad .$$

We then apply the good conductor approximation $\beta\Delta >> 1$ use asymptotic approximations for the modified Bessel functions

$$I_0(x) \approx \frac{e^x}{\sqrt{2\pi x}}\left[1+\frac{1}{8x}+\frac{9}{128x^2}+\frac{75}{1024x^3}+....\right] \quad \text{for } x>>1$$

$$I_1(x) \approx \frac{e^x}{\sqrt{2\pi x}}\left[1-\frac{3}{8x}-\frac{15}{128x^2}-\frac{105}{1024x^3}-....\right] \quad \text{for } x>>1$$

to obtain a simplified result for the initial tern in the convolution

$$E_0(t) \approx J(t)\int_{\beta\Delta}^{\infty} dv\, Z_1(v) \approx \frac{J(t)}{\sqrt{2\pi\beta\Delta}}\left[1+\frac{1}{8\beta\Delta}+\frac{9}{128(\beta\Delta)^2}+....\right].$$

For the remaining convolution terms $E_1(t)$ through $E_M(t)$ we can derive a recurrence relation. Taking J(t) to be nearly constant within each time step, we write for $n > 1$

$$E_m(n\Delta) \equiv \int_0^{(n-1)\Delta} du\, \beta\, c_m \exp(-\beta(n\Delta-u))\, J(u)$$

$$= c_m \int_0^{(n-1)\Delta} du\, \beta \exp(-\omega_m\beta(n\Delta-u))\, J(u)$$

$$= c_m \sum_{k=1}^{n-1} \int_{(k-1)\Delta}^{k\Delta} du\, \beta \exp(-\omega_m\beta(n\Delta-u))\, J(k\Delta)$$

$$= \frac{c_m}{\omega_m}\sum_{k=1}^{n-1} \exp(-\omega_m\beta(n-k)\Delta)\,[1-\exp((-\omega_m\beta\Delta)]\, J(k\Delta)$$

$$= \exp(-\omega_m\beta\Delta)\frac{c_m}{\omega_m}\sum_{k=1}^{n-2} \exp(-\omega_m\beta(n-k)\Delta)\,[1-\exp((-\omega_m\beta\Delta)]\, J(k\Delta)$$

$$+\frac{c_m}{\omega_m}\exp(-\omega_m\beta\Delta)[1-\exp((-\omega_m\beta\Delta)]\, J((n-1)\Delta)$$

$$= \exp(-\omega_m\beta\Delta)E_m((n-1)\Delta)+\frac{c_m}{\omega_m}\exp(-\omega_m\beta\Delta)[1-\exp((-\omega_m\beta\Delta)]\, J((n-1)\Delta)$$

The recurrence relation involves only the values of the convolution term E_m and the surface current J at the previous time step $(n-1)\Delta$. A similar recurrence relation can be developed for the convolution of Y(t) with the current. Since there are only M terms that need to be updated at each space-time point, we have reduced the added computational complexity of the convolution from a factor of order N_t to a factor of order $\log(N_t)$.

SECTION 5

IMPLEMENTATION FOR A LOSSY 2-D PLANAR TRANSMISSION LINE

In this section we illustrate the efficient solution for a specific problem and develop the numerical equations in detail. We have chosen a two-dimensional (2D) rather than a three-dimensional problem, not only because of our limited computational resources, but also because we desire a problem with an analytical solution that can validate the efficient MFIE solution.

The lossy 2D planar transmission line illustrated in Figure 5-1 has a well-established analytical solution [20]. The line consists of a free-space region located between two thick planes of a lossy conductor with dielectric constant ε_0 and conductivity σ. The volumes are separated by a gap a in the x-direction, the y-coordinate ignorable, i.e., $\partial/\partial y = 0$, and propagation is in the z-direction. All fields are zero before t = 0, when a driving current $J_0(t)\hat{\mathbf{x}}$ is applied across the gap at the location z = 0. Waves will propagate in the $\pm\hat{\mathbf{z}}$ directions with surface current $\pm J_S(z,t)\hat{\mathbf{z}}$ on the upper surface at x = +a/2 and $\mp J_S(z,t)\hat{\mathbf{z}}$ on the lower surface at a = -a/2. Because of this symmetry we only need to solve $J_S(z,t)$ for observation points at x = a/2 and z > 0. The actual field components are H_y, E_x, and E_z, but these are secondary variables that are derivable from the solution $J_S(z,t)$. We numerically implement only the MFIE, which is preferable to the EFIE for this type of problem. Taking $\varepsilon_c = \varepsilon = \varepsilon_0$, $\mu_c = \mu = \mu_0$, $\Omega = 2\pi$, and $\nabla \times \hat{\mathbf{z}} J(z,t) = 0$, the MFIE for the 2D planar problem becomes

$$\mathbf{J}_S = 2\,\mathbf{n}\times\mathbf{H}^{inc} + \frac{\mathbf{n}}{2\pi}\times\oint_S ds' \int dt' \frac{\delta(t'-t+R/c)}{R}\left\{\left[\frac{1}{R}+\frac{1}{c}\frac{\partial}{\partial t'}\right]\mathbf{J}_S'\times\hat{\mathbf{R}} + \frac{1}{c}\frac{\partial}{\partial t'}Z'*(\mathbf{n}'\times\mathbf{J}_S')\right\}.$$

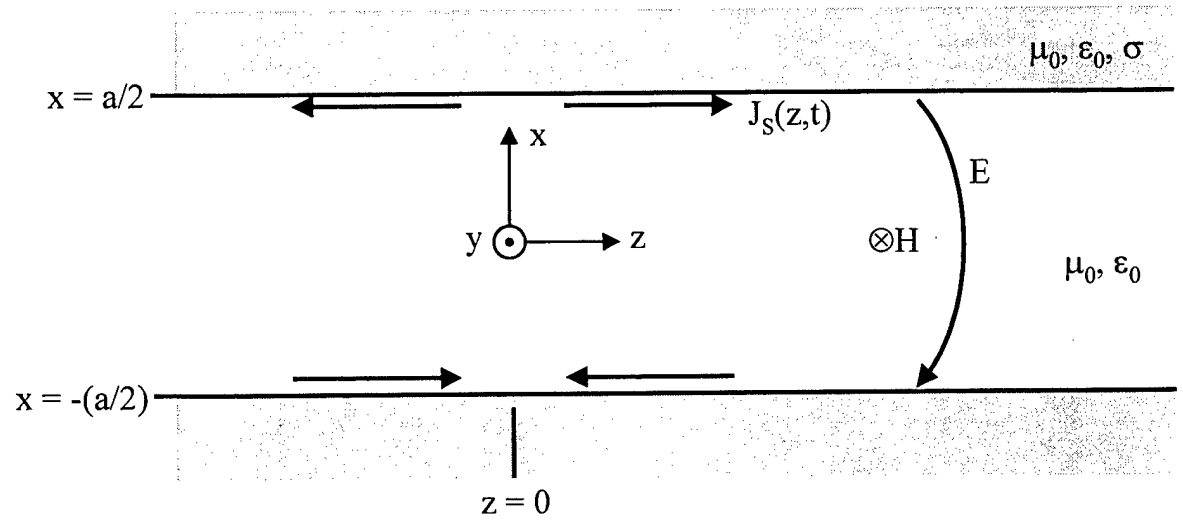

Figure 5-1. Geometry for 2D planar transmission line.

The incident field $\mathbf{H}^{inc}(z,t)$ results from the current applied at the plane z = 0 in the absence of the conductors at x = ±a/2. Although we could have generated the incident magnetic field by a current applied on a conductor closing the gap at z = 0, it is numerically easier to apply twice the current across free space, which gives the symmetric waves traveling $\pm\hat{\mathbf{z}}$ directions. The incident magnetic field $H^{inc}(r,t)$ is given by the vector potential

$$\mathbf{H}^{inc}(\mathbf{r},t) = \nabla \times \mathbf{A}^{inc}(\mathbf{r},t)$$

where the time-domain vector potential for a sheet current $2J_0$ at z' = 0 and |x'| < a/2 is given by

$$\mathbf{A}^{inc}(\mathbf{r},t) = \frac{1}{4\pi}\int_{-a/2}^{a/2} dx' \int_{-\infty}^{\infty} dy' \int_{0}^{\infty} dt' \frac{\delta(t'-t+R/c)}{R} 2J_0(t)\hat{\mathbf{x}} \quad .$$

The incident surface current on the surface at x = a/2 is then given by

$$\begin{aligned}
\mathbf{J}^{inc}(z,t) = \mathbf{n}\times\mathbf{H}^{inc}(\mathbf{r},t) &= -\frac{\hat{\mathbf{x}}}{4\pi}\times \int_{-a/2}^{a/2} dx' \int_{-\infty}^{\infty} dy' \int_{0}^{\infty} dt' \, \nabla \frac{\delta(t'-t+R/c)}{R} \times \hat{\mathbf{x}}\, 2J_0(t') \\
&= -\frac{\hat{\mathbf{x}}}{2\pi}\times \int_{-a/2}^{a/2} dx' \int_{-\infty}^{\infty} dy' \int_{0}^{\infty} dt' \left[-\frac{\delta(t'-t+R/c)}{R^2} + \frac{\delta'(t'-t+R/c)}{cR} \right] \hat{\mathbf{R}}\times\hat{\mathbf{x}} J_0(t') \\
&= \frac{\hat{\mathbf{x}}}{2\pi}\times \int_{-a/2}^{a/2} dx' \int_{-\infty}^{\infty} dy' \int_{0}^{\infty} dt' \left[\frac{J_0(t')}{R^2} + \frac{\partial J_0(t')}{cR\,\partial t'} \right] \frac{(a/2-x')\hat{\mathbf{x}} + (y-y')\hat{\mathbf{y}} + z\hat{\mathbf{z}}}{R} \times \hat{\mathbf{x}}\, \delta(t'-t+R/c) \\
&= \frac{\hat{\mathbf{z}}}{2\pi} \int_{-a/2}^{a/2} dx' \int_{-\infty}^{\infty} dy' \int_{0}^{\infty} dt' \left[-\frac{J_0(t')}{R^2} + \frac{\partial J_0(t')}{cR\,\partial t'} \right] \frac{z}{R} \delta(t'-t+R/c) \\
&\equiv \hat{\mathbf{z}}\, J^{inc}(z,t) \quad ,
\end{aligned}$$

where we have used the fact that that the (y-y') component of **R** is odd and vanishes when the y' integration is carried out.

Returning to the vector MFIE, we perform the vector algebra to reduce the MFIE to a scalar equation. Since the unit normal **n** points into the gap, the first vector product gives

$$\begin{aligned}
x' = +a/2: \quad & \mathbf{n}\times(\mathbf{J}'\times\mathbf{R}) = (-\hat{\mathbf{x}})\times(\hat{\mathbf{z}}J'\times(\mathbf{y}-\mathbf{y}'+\mathbf{z}-\mathbf{z}')) = \hat{\mathbf{x}}\times\hat{\mathbf{x}}J'\times(y-y')J' = 0 \\
x' = -a/2: \quad & \mathbf{n}\times(\mathbf{J}'\times\mathbf{R}) = (-\hat{\mathbf{x}})\times(-\hat{\mathbf{z}}J')\times(a\hat{\mathbf{x}}+\mathbf{y}-\mathbf{y}'+\mathbf{z}-\mathbf{z}')) = \hat{\mathbf{x}}\times\hat{\mathbf{y}}aJ' = \hat{\mathbf{z}}aJ' \quad .
\end{aligned}$$

The second vector product gives

$$\begin{aligned}
x' = +a/2: \quad & \mathbf{n}\times(\mathbf{n}'\times\mathbf{J}') = (-\hat{\mathbf{x}})\times(-\hat{\mathbf{x}}\times\hat{\mathbf{z}}J') = (-\hat{\mathbf{x}})\times(\hat{\mathbf{y}}J') = -\hat{\mathbf{z}}J' \\
x' = -a/2: \quad & \mathbf{n}\times(\mathbf{n}'\times\mathbf{J}') = (-\hat{\mathbf{x}})\times(\hat{\mathbf{x}}\times(-\hat{\mathbf{z}}J')) = (-\hat{\mathbf{x}})\times(\hat{\mathbf{y}}J') = -\hat{\mathbf{z}}J' \quad .
\end{aligned}$$

Thus all terms have only $\hat{\mathbf{z}}$ components and we obtain a scalar integral equation

$$J(z,t) = 2J^{inc}(z,t) + J_1(z,t) - J_2(z,t) - J_3(z,t)$$

where the individual terms are given by

$$J^{inc}(z,t)=\frac{1}{2\pi}\int_{-a/2}^{a/2}dx'\int_{-\infty}^{\infty}dy'\int_{0}^{\infty}dt'\frac{z}{R}\,\delta(t'-t+R/c)\left[-\frac{J_0(t')}{R^2}+\frac{\partial J_0(t')}{cR\,\partial t'}\right],\ R^2=(\frac{a}{2}-x')^2+(y-y')^2+z^2$$

$$J_1(z,t)\equiv\frac{1}{2\pi}\int_{-\infty}^{\infty}dz'\int_{-\infty}^{\infty}dy'\int dt'\frac{\delta(t'-t+R/c)}{R}\left\{\left[\frac{1}{R}+\frac{1}{c}\frac{\partial}{\partial t'}\right]\frac{a}{R}J'(z',t')\right\},\ R^2=(\frac{a}{2})^2+(y-y')^2+(z-z')^2$$

$$J_2(z,t)\equiv\frac{1}{2\pi}\int_{-\infty}^{\infty}dz'\int_{-\infty}^{\infty}dy'\int dt'\frac{\delta(t'-t+R/c)}{R}\left\{\frac{1}{c}\frac{\partial}{\partial t'}Z'(t')*J'(z',(t')\right\},\ R^2=(\frac{a}{2})^2+(y-y')^2+(z-z')^{2^2}$$

$$J_3(z,t)\equiv\frac{1}{2\pi}\int_{-\infty}^{\infty}dz'\int_{-\infty}^{\infty}dy'\int dt'\frac{\delta(t'-t+R/c)}{R}\left\{\frac{1}{c}\frac{\partial}{\partial t'}Z'(t')*J'(z',t')\right\},\ R^2=(y-y')^2+(z-z')^2$$

Each of these terms contains a y' integration where y' appears only in R. Without loss of generality we take y = 0 and change the integration variable from y' to R

$$\int_{-\infty}^{\infty}dy'\frac{\delta(t'-t+R/c)}{R^n}=2\int_0^{\infty}dR\,\frac{\delta(t'-t+R/c)}{R^{n-1}\sqrt{R^2-(x-x')^2-(z-z')^2}}$$

$$=\frac{2}{[c\,|t-t'|]^{n-1}}\frac{c}{\sqrt{c^2(t-t')^2-(x-x')^2-(z-z')^2}}\int_0^{\infty}dR\,\delta(R-c(t-t'))$$

$$=\begin{cases}\dfrac{2}{[c\,|t-t'|]^{n-1}}\dfrac{c}{\sqrt{c^2(t-t')^2-(x-x')^2-(z-z')^2}} & \text{if}\quad c(t-t')>\sqrt{(x-x')^2+(z-z')^2}\\ 0\quad\text{otherwise}\end{cases}.$$

This result is consistent with the 2D Green's function, whose time dependence has an inverse square root rather than a delta function [12].

Thus the $J^{inc}(z,t)$ term becomes, after performing the y' integration,

$$J^{inc}(r,t)=\frac{z}{2\pi}\int_{x\,min}^{a/2}dx'\int_0^t dt'\left[-\frac{J_0(t')}{c^2(t-t')^2}+\frac{1}{c^2(t-t')}\frac{\partial J_0(t')}{\partial t'}\right]\frac{2c}{\sqrt{c^2(t-t')^2-(a/2-x')^2-z^2}}$$

where the integral limits are determined by the requirement that $c^2(t-t')^2-(a/2-x')^2-z^2>0$, i.e.,

$$x>x_{min}\equiv\max\begin{cases}a/2-\sqrt{c^2(t-t')^2-z^2}\\ -a/2\end{cases}.$$

This result can be further simplified by changing variables to u = c(t-t') and v = x'-a/2,

$$J^{inc}(r,t)=\frac{z}{\pi}\int_0^{ct}du\left[-\frac{J_0(t-u/c)}{u^2}-\frac{\partial J_0(t-u/c)}{u\,\partial u}\right]F(u)\quad,$$

$$F(u)\equiv\int_0^{v\,min}dx'\frac{1}{\sqrt{u^2-v^2-z^2}}=\sin^{-1}\left(\frac{a}{v_{max}}\right)\quad,\quad v_{max}\equiv\min\begin{cases}a\\ \sqrt{u^2-z^2}\end{cases}.$$

Integrating the derivative term by parts,

$$\int_z^{ct} du \left[\frac{\partial J_0(t-u/c)}{\partial u}\right]\frac{F(u)}{u} = \left[J_0(t-u/c)\frac{F(u)}{u}\right]_z^{ct} - \int_z^{ct} du\, J_0(t-u/c)\left[\frac{\partial F(u)}{u\,\partial u} - \frac{F(u)}{u^2}\right]$$

$$= -\frac{\pi}{2z}J_0(t-z/c) + \int_z^{ct} du\, J_0(t-u/c)\frac{F(u)}{u^2} - \int_z^{ct} du\, J_0(t-u/c)\frac{\partial F(u)}{u\,\partial u}$$

For $u^2 < a^2 + z^2$ we have $v_{max} = a$ and F = constant. Thus $\partial F/\partial u$ is non-vanishing only for $u^2 > a^2 + z^2$, where

$$\frac{\partial F(u)}{\partial u} = \frac{\partial}{\partial u}\sin^{-1}\left(\frac{a}{\sqrt{u^2-z^2}}\right) = \frac{1}{\sqrt{1-a^2/(u^2-z^2)}}\frac{-au}{\sqrt{(u^2-z^2)^3}} = -\frac{au}{(u^2-z^2)\sqrt{u^2-z^2-a^2}}\ .$$

Combining the above results we obtain the incident field

$$J^{inc}(z,t) = \frac{1}{2}J_0(t-z/c) - \frac{za}{\pi}\int_\alpha^{ct} du\ \frac{J_0(t-u/c)}{(u^2-z^2)\sqrt{u^2-z^2-a^2}}$$

$$\alpha \equiv \sqrt{a^2+z^2}\,.$$

Thus $J^{inc}(z,t)$ vanishes for $z > ct$, because $J_0(t)$ vanished for $t \le 0$. Taking $J_0(t)$ to be piecewise linear, we can rewrite the incident field as a sum of separate integrals over each time step

$$J^{inc}(z,t) = \frac{1}{2}J_0(t-z/c) - \frac{z}{\pi c\Delta}\sum_{u=\alpha+c\Delta}^{ct}\left[J_0(t-u/c) - J_0(t-u/c+\Delta)\right]\left[F_1(u) - F_1(u-c\Delta)\right]$$

$$-\frac{1}{2\pi c\Delta}\sum_{u=\alpha+c\Delta}^{ct}\left[(c\Delta-u)J_0(t-u/c) + u\,J_0(t-u/c+\Delta)\right]\left[F_0(u) - F_0(u-c\Delta)\right]$$

$$F_0(u) \equiv \int^u \frac{2za\,du}{(u^2-z^2)\sqrt{u^2-z^2-a^2}} = \sin^{-1}\left(\frac{z^2-a^2-2a^2z^2/(u^2-z^2)}{z^2+a^2}\right)$$

$$F_1(u) \equiv \int^u \frac{au\,du}{(u^2-z^2)\sqrt{u^2-z^2-a^2}} = \tan^{-1}\left(\sqrt{\frac{u^2-z^2}{a^2}-1}\right)$$

The $J_1(z,t)$ term becomes, after performing the y' integration,

$$J_1(z,t) = \frac{a}{\pi}\int_{z\,min}^{z\,max} dz' \int_0^{t-\alpha_1} dt' \left[\frac{J(z',t')}{c^2(t-t')^2} + \frac{1}{c^2(t-t')}\frac{\partial J(z',t')}{\partial t'}\right]\frac{c}{\sqrt{c^2(t-t')^2-\alpha_1^2}}\ ,$$

The finite limits on the z' integration arise because the incident current $J^{inc}(z,t)$ and consequently the total surface current J(z,t) are identically zero unless $t > z$. Physically, the sum of the propagation time of the incident wave from the origin to the source point z' plus the additional propagation time from the source point to the observation point z must be less than t in order for get a non-zero contribution to J(z,t), i.e.,

$$|z'| + \sqrt{(z-z')^2 + (x-x')^2} \le ct .$$

It is then straightforward to show that the z' integrand vanishes outside the interval $[z_{min}, z_{max}]$, where

$$z_{max} \equiv \frac{t^2 - z^2 - (x-x')^2}{2(t-z)}$$

$$z_{min} \equiv -\frac{t^2 - z^2 - (x-x')^2}{2(t+z)} .$$

Next we change the time variable to $u \equiv c(t-t')$ and integrate by parts to remove the $(t-t')^{-2}$ singularity,

$$J_1(z,t) = \frac{a}{\pi} \int_{z_{min}}^{z_{max}} dz' \int_0^{t-\alpha_1} dt' \left[\frac{J(z',t')}{c^2(t-t')^2} + \frac{1}{c^2(t-t')} \frac{\partial J(z',t')}{\partial t'} \right] \frac{c}{\sqrt{c^2(t-t')^2 - \alpha_1^2}}$$

$$= \frac{a}{\pi} \int_{z_{min}}^{z_{max}} dz' \int_{c\alpha_1}^{ct} du \left[\frac{J(z',t-u/c)}{u^2} + \frac{1}{cu} \frac{\partial J(z',t-u/c)}{\partial t'} \right] \frac{1}{\sqrt{u^2 - \alpha_1^2}}$$

$$= \frac{a}{\pi} \int_{z_{min}}^{z_{max}} dz' \left\{ \left[\frac{\sqrt{u^2 - \alpha_1^2}}{\alpha_1^2 u} J(z',t-u) \right]_{c\alpha_1}^{ct} + \int_{c\alpha_1}^{ct} du \frac{\partial J(z',t-u)}{c\,\partial t} \left[\frac{\sqrt{u^2 - \alpha_1^2}}{u\,\alpha_1^2} + \frac{1}{u\sqrt{u^2 - \alpha_1^2}} \right] \right\}$$

$$= \frac{a}{\pi} \int_{z_{min}}^{z_{max}} dz' \int_{c\alpha_1}^{ct} du \frac{\partial J(z',t-u)}{c\,\partial t} \frac{u}{\alpha_1^2 \sqrt{u^2 - \alpha_1^2}} .$$

Next we take J(z',t') to be piecewise linear from one time point to the next so that the slope is constant within each time interval $[t', t'+\Delta]$. Then we can write the u-integral as a sum of integrals with $\partial J / \partial t$ outside of each time integral,

$$J_1(z,t) = \frac{a}{\pi} \int_{z_{min}}^{z_{max}} dz' \sum_{u=\alpha_1}^{t-\Delta} \frac{J(z',t-u/c) - J(z',t-u/c-\Delta)}{c\,\Delta} \int_u^{u+c\Delta} du \frac{u}{\alpha_1^2 \sqrt{u^2 - \alpha_1^2}}$$

$$= \frac{a}{\pi} \int_{z_{min}}^{z_{max}} dz' \sum_{u=\alpha_1}^{t-\Delta} \frac{J(z',t-u/c) - J(z',t-(u/c+\Delta))}{c\,\Delta} \left[\frac{\sqrt{u^2 - \alpha_1^2}}{\alpha_1^2} \right]_u^{u+c\Delta}$$

$$= \frac{a}{\pi} \int_{z_{min}}^{z_{max}} dz' \sum_{u=\alpha_1}^{t-\Delta} \frac{J(z',t-u/c) - J(z',t-(u/c+\Delta))}{c\,\Delta} \frac{\sqrt{(u+c\Delta)^2 - \alpha_1^2} - \sqrt{u^2 - \alpha_1^2}}{\alpha_1^2} .$$

The z' integrand is a complicated function of z' because a_1 depends upon z', so we will evaluate it numerically rather than analytically. Using the trapezoidal rule with a step size $c\Delta$ that meets the stability criterion $\delta R \le c\delta t$, we obtain

$$J_1(z,t) = \frac{a}{\pi} \sum_{z'=z_{min}}^{z_{max}} \phi(z') \sum_{u=\alpha_1}^{t-\Delta} [J(z',t-u/c) - J(z',t-(u/c+\Delta))] \frac{\sqrt{(u+c\Delta)^2-\alpha_1^2} - \sqrt{u^2-\alpha_1^2}}{\alpha_1^2} \quad ,$$

where we have omitted the 0.5 factor for the end terms because the integrand actually vanishes there. We have also included the factor

$$\phi(z') = \begin{cases} 1 & \text{for } z' > 0 \\ 0 & \text{for } z' = 0 \\ -1 & \text{for } z' < 0 \end{cases}$$

since J(z',t') changes sign at z' = 0, which also results in a null contribution at z' = 0.

The $J_2(z,t)$ term becomes, after performing the y' integration, ,

$$J_2(z,t) \equiv \frac{1}{\pi} \int_{z\,min}^{z\,max} dz' \int_0^{t-\alpha 1} dt' \frac{1}{c} \frac{\partial}{\partial t'} Z(t') * J(z',t') \frac{c}{\sqrt{c^2(t-t')^2 - \alpha_1^2}}$$

$$\text{where} \quad \alpha_1 \equiv \sqrt{(x-x')^2 + (z-z')^2} \quad .$$

Then writing E(z',t') = Z(t') * J(z',t') to simplify the notation, the evaluation of $J_2(z,t)$ proceeds in a manner similar to $J_1(z,t)$ except that no integration by parts is needed,

$$J_2(z,t) = \frac{1}{\pi} \int_{z_{min}}^{z_{max}} dz' \int_0^{t-\alpha_1} dt' \frac{\partial E(z',t')}{c\partial t'} \frac{c}{\sqrt{c^2(t-t')^2 - \alpha_1^2}}$$

$$= \frac{1}{\pi} \int_{z_{min}}^{z_{max}} dz' \int_{c\alpha_1}^{ct} du \frac{\partial E(z',t-u/c)}{c\,\partial t} \frac{1}{\sqrt{u^2-\alpha_1^2}}$$

$$= \frac{1}{\pi} \int_{z_{min}}^{z_{max}} dz' \sum_{u\,=\,c\alpha_1}^{c(t-\Delta)} \frac{E(z',t-u/c) - E(z',t-u/c-\Delta)}{c\,\Delta} \int_u^{u+c\Delta} du \frac{1}{\sqrt{u^2-\alpha_1^2}}$$

$$= \frac{1}{\pi} \int_{z_{min}}^{z_{max}} dz' \sum_{u\,=\,c\alpha_1}^{c(t-\Delta)} \frac{E(z',t-u/c) - E(z',t-u/c-\Delta)}{c\,\Delta} \left[\cosh^{-1}\left(\frac{u}{\alpha_1}\right) \right]_u^{u+c\Delta}$$

$$= \frac{1}{\pi} \sum_{z'\,=\,z_{min}}^{z_{max}} \text{sign}(z') \sum_{u\,=\,c\alpha_1}^{c(t-\Delta)} [E(z',t-u/c) - E(z',t-u/c-\Delta)] \left[\cosh^{-1}\left(\frac{u+c\Delta}{\alpha_1}\right) - \cosh^{-1}\left(\frac{u}{\alpha_1}\right) \right] \quad .$$

It is important to note that the summations in $J_1(z,t)$ and $J_2(z,t)$ involve only J(z',t')) terms occurring at t' < t, because the observation point is separated from the source points by at least the gap spacing a.

Evaluation of $J_3(z,t)$ proceeds in a manner similar to $J_2(z,t)$ but with α_1 replaced by α_0. Special care is needed, however, to treat the integrable singularity on the "self-patch" where z' ≈ z and t' ≈ t. Thus we write

$$J_3(z,t) = J_3^s(z,t) + J_3^{ns}(z,t)$$

where the "non-self" term follow from $J_2(z,t)$

$$J_3^{ns}(z,t) = \frac{1}{\pi} \sum_{z'=z_{min}}^{z_{max}} \text{sign}(z') \sum_{u=c\alpha_0>0}^{c(t-\Delta)} [E(z',t-u/c) - E(z',t-u/c-\Delta)] \times \left[\cosh^{-1}\left(\frac{u+c\Delta}{\alpha_1}\right) - \cosh^{-1}\left(\frac{u}{\alpha_1}\right) \right]$$

$$\alpha_0 \equiv |z-z'|$$

and the self–patch term is given by

$$J_3^s(z,t) \equiv \frac{1}{\pi} \frac{\partial E(z,t)}{c\partial t} \int_{z-c\Delta/22}^{z+c\Delta/2} dz' \int_{|z'-z|}^{c\Delta} du \frac{1}{\sqrt{u^2-(z'-z)^2}}$$

$$= \frac{[E(z,t)-E(z,t-\Delta)]}{c\Delta} \frac{2}{\pi} \int_0^{c\Delta/2} dv \int_v^{c\Delta} du \frac{1}{\sqrt{u^2-v^2}}$$

$$= \frac{[E(z,t)-E(z,t-\Delta)]}{c\Delta} \frac{2}{\pi} \int_0^{c\Delta/2} dv \, \text{sech}^{-1}\left(\frac{v}{c\Delta}\right)$$

$$= \frac{[E(z,t)-E(z,t-\Delta)]}{c\Delta} \frac{2}{\pi} \left[v \, \text{sech}^{-1}\left(\frac{v}{c\Delta}\right) + c\Delta \sin^{-1}\left(\frac{v}{c\Delta}\right) \right]_0^{c\Delta/2}$$

$$= [E(z,t)-E(z,t-\Delta)] \left[\frac{\ln(2+\sqrt{3})}{\pi} + \frac{1}{3} \right]$$

$$= \left[\frac{J(z,t)-J(z,t-\Delta)}{\sqrt{2\pi\beta\Delta}} - \sum_{m=1}^{M} [E_m(z,t)-E_m(z,t-\Delta)] \right] \kappa,$$

$$\kappa \equiv \left[\frac{\ln(2+\sqrt{3})}{\pi} + \frac{1}{3} \right].$$

Notice that the self-patch term now contains a term in J(z,t) that must be moved to the left hand side of the MFIE. Thus, the time-stepping solution can be written

$$J(z,t) = \frac{J^{inc}(z,t) + J_1(z,t) - J_2(z,t) - J_3^{ns}(z,t) + \kappa \left[\frac{J(z,t-\Delta)}{\sqrt{2\pi\beta\Delta}} + \sum_{m=1}^{M} [E_m(z,t)-E_m(z,t-\Delta)] \right]}{1 + \frac{\kappa}{\sqrt{2\pi\beta\Delta}}}$$

where all the terms on the right involve J(z't') for earlier times t' < t.

SECTION 6

COMPARISON WITH ANALYTIC SOLUTION

In this section we will validate the efficient MFIE solution of the previous section against an analytical solution of the same problem. We find good agreement bewteen the solutions in both time and frequency domains.

Ramo Whinnery and van Duzer [20] present an accessible treatment of the lossy 2D planar transmission line in the frequency domain. For a wave propagating in the +z direction as $\exp(j\omega t-\gamma z)$ the in a line with $\mu_c = \mu$ and $\varepsilon_c = \varepsilon$, the propagation constant is given by

$$\gamma^2 = -k^2\left[1-j(j+1)\frac{\delta}{a}\right], \quad \delta \equiv \sqrt{\frac{2}{\mu_c\omega\sigma_c}} \quad , \quad k \equiv \frac{\omega}{c} \ ,$$

where δ is the skin depth at frequency ω. The surface impedance boundary condition (SIBC) already requires $\delta/a \ll 1$, so the propagation constant can be simplified to

$$\gamma \approx jk\left[1-j(j+1)\frac{\delta}{2a}\right] = k\frac{\delta}{2a} + jk\left[1+\frac{\delta}{2a}\right].$$

Thus, an initial frequency component $\tilde{J}_0(\omega)\, e^{j\omega t}$ becomes $\tilde{J}_0(\omega) e^{j\omega t-\gamma z}$ after propagating a distance z in the lossy line. The real part of γ causes attenuation, while the imaginary part gives an increase in the wave number that reduces the propagation speed. We then use the inverse fast Fourier transform to obtain the analytic solution in the time domain for comparison to the efficient MFIE solution. Conversely, we also performed a fast Fourier transform of the efficient MFIE solution for comparison with the analytic solution in the frequency-domain.

Before proceeding with the comparison of the analytic and efficient MFIE solutions, it is important to relate the time-domain good conductor requirement

$$\beta\Delta >> 1$$

to the SIBC (small skin depth requirement) and another requirement used in the derivation of the analytic result for the propagation constant γ, i.e.,

$$\frac{\delta}{a} << 1 \quad \text{and} \quad \frac{a}{\delta}\frac{\varepsilon\omega}{\sigma\sqrt{2}} << 1 \ ,$$

respectively. For a time-domain computation running to $N_t\Delta$, the relevant frequency range is

$$\frac{1}{N_t\Delta} \le f \le \frac{1}{4\Delta} \quad \text{or} \quad \frac{2\pi}{N_t\Delta} \le \omega \le \frac{2}{\pi\Delta} \ ,$$

so the SIBC and analytic requirements respectively become

$$\sqrt{\beta\Delta} >> \frac{c\Delta}{a}\sqrt{\frac{N_t}{2\pi}} \quad \text{and} \quad \sqrt{\beta\Delta} >> \frac{a}{c\Delta}\frac{1}{\pi^{3/2}} \ .$$

For $N_t = 160$ and $a = 3c\Delta$ we have chosen $\beta\Delta = 1000$ so that both inequalities are satisfied by least a factor of 20. It is important to note that the efficient integral equation approach in general requires only the easily-satisfied requirement

$$\sqrt{\beta\Delta} >> \frac{c\Delta}{a}\sqrt{\frac{N_t}{2\pi}} \quad ,$$

where a is the smallest geometric scale length of the problem.

For the comparisons we have redefined the physical units so that all computational variables are dimensionless, i.e., $c = 1$, $\varepsilon = 1$, $\mu = 1$, $\Delta = 1$. The driving current was taken to be a gaussian modified by a (1 + cos) factor to give a cutoff at $t = 40\Delta$,

$$J_0(t) = \begin{cases} 0.5\exp\left(-\left(\frac{t-20\Delta}{8\Delta}\right)^2\right)\left[1+\cos\left(\pi\left(\frac{t}{20\Delta}-1\right)\right)\right], & 0 \le t \le 40\Delta \\ 0 \quad , \quad \text{otherwise.} \end{cases}$$

We also used a bipolar shape for the driving current

$$J_0(t) = \begin{cases} \exp\left(-\left(\frac{t-20\Delta}{8\Delta}\right)^2\right)\left[1+\cos\left(\pi\left(\frac{t}{20\Delta}-1\right)\right)\right]\sin\left(\pi\left(\frac{t}{20\Delta}-1\right)\right), & 0 \le t \le 40\Delta \\ 0 \quad , \quad \text{otherwise,} \end{cases}$$

which was then normalized to give a peak value of 1. Although both the monopolar and bipolar pulse shapes are continuous and differentiable at $t = 0$ and $t = 40\Delta$, the higher order derivatives are discontinuous at those times.

We first calculate the evolution of the monopolar pulse in an ideal (non-lossy) line. Figure 6-1 shows the evolution of the pulse in the time domain as it passes various locations in the line. As expected for an ideal line, the pulse propagates with no change in shape. Figure 6-2 compares the magnitude of the initial frequency spectrum at $z = 0$ with that off the pulse shape at $z = 120c\Delta$. We find excellent agreement out to a frequency of about $0.16/\Delta$, where both the initial and propagated spectra depart from the smooth decay of the lower-frequency spectrum. This feature is due to the temporal cutoff, which as we noted above is not perfectly smooth. The transition occurs not at a given frequency, but rather when the spectral amplitude reaches a low level comparable to the magnitude of the time-domain points adjacent to the cutoff.

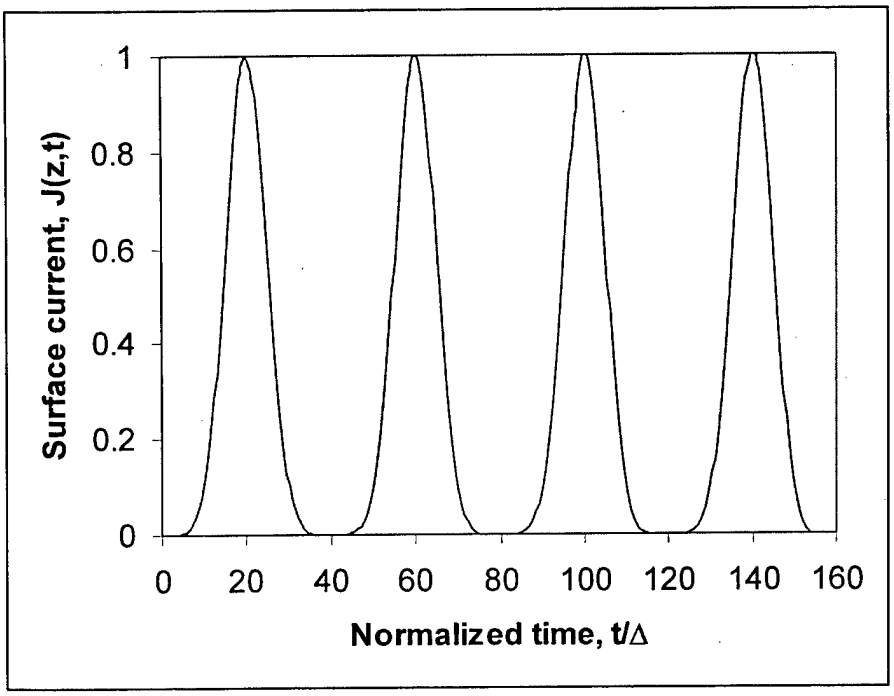

Figure 6-1. Time-domain propagation of a monopolar pulse in an ideal transmission line at locations z = 0, 40cΔ, 80cΔ, & 120cΔ using the MFIE solution.

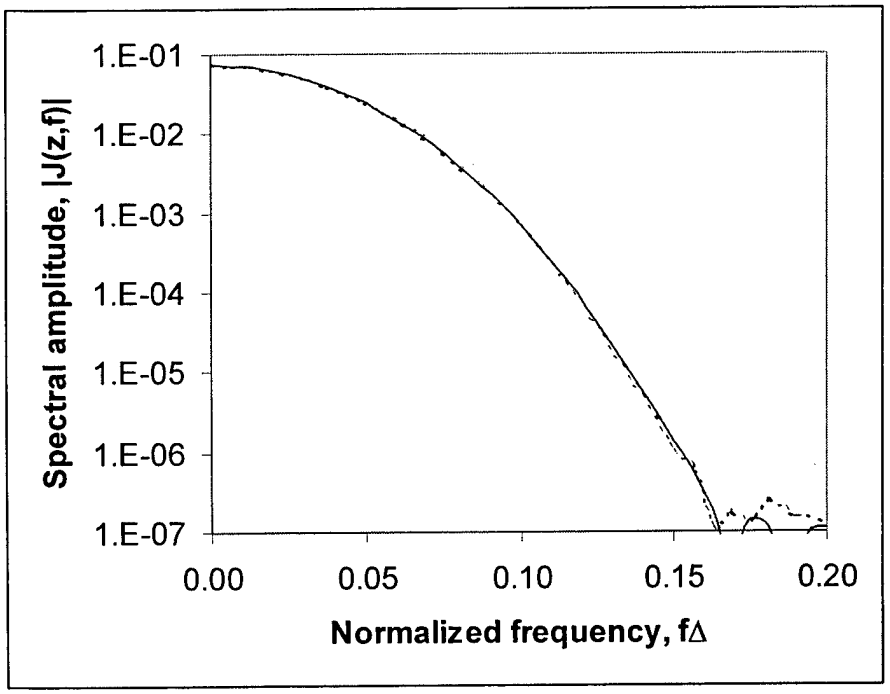

Figure 6-2. Frequency spectra of a monopolar pulse propagated in an ideal transmission line at z = 0 (solid line) and z = 120cΔ (dashed line).

Next we treat the lossy transmission line, for which we use the bipolar pulse. The monopolar pulse has a zero-frequency component, which has an infinite skin depth that violates the SIBC requirement. We have chosen $\beta\Delta = 1000$ and 10 terms for the recursive convolution. Figure 6-3 shows good agreement between the analytic and efficient MFIE pulse shapes at various positions along the line. As expected the pulse width increases, the pulse height decreases, and the propagation speed (see the zero-crossing) is slightly less than $c = 1$. It is important to note that both analytic and efficient MFIE solutions have a slowly decaying wake, so that any finite-time calculation will be non-zero at $t = N_t\Delta$. The cutoff of this wake by the finite fast Fourier transform will always introduce artifacts into the frequency spectrum

For the frequency domain, Figure 6-4 compares the analytic and efficient MFIE spectral amplitudes at $z = 0, 40\Delta, \& 80\Delta$. Again the agreement is good at lower frequencies, but the temporal cutoffs cause a raised spectral plateau at high frequency. The plateau is higher for $z = 80c\Delta$ than for $40c\Delta$, because the former waveform has less time than the latter for the wake to decay. The frequency-domain attenuation curves provide a more sensitive comparison of the analytic and efficient MFIE solutions. Figure 6-5 shows good agreement at frequencies below the cutoff, which is really an artifact of the finite time window for the MFIE computation.

Thus we conclude that the surface impedance boundary condition with a recursive convolution is a valid approach for the solution of dispersive time-domain integral equations.

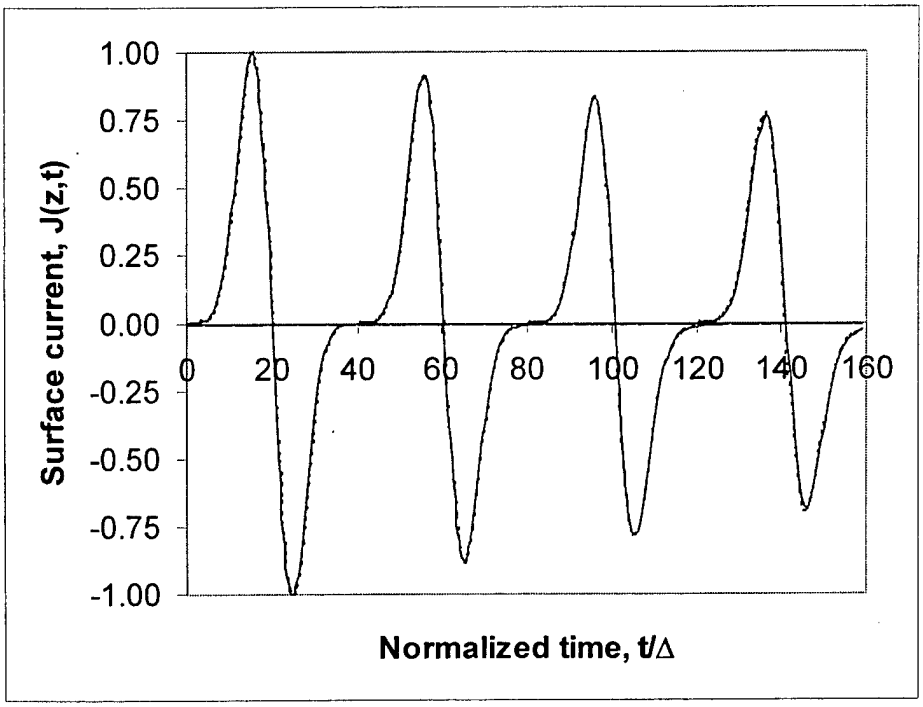

Figure 6-3. Time-domain propagation of a bipolar pulse in a lossy transmission line at locations $z = 0, 40\ c\Delta, 80\ c\Delta, \& 120\ c\Delta$; solid line is analytic and dashed line is efficient MFIE.

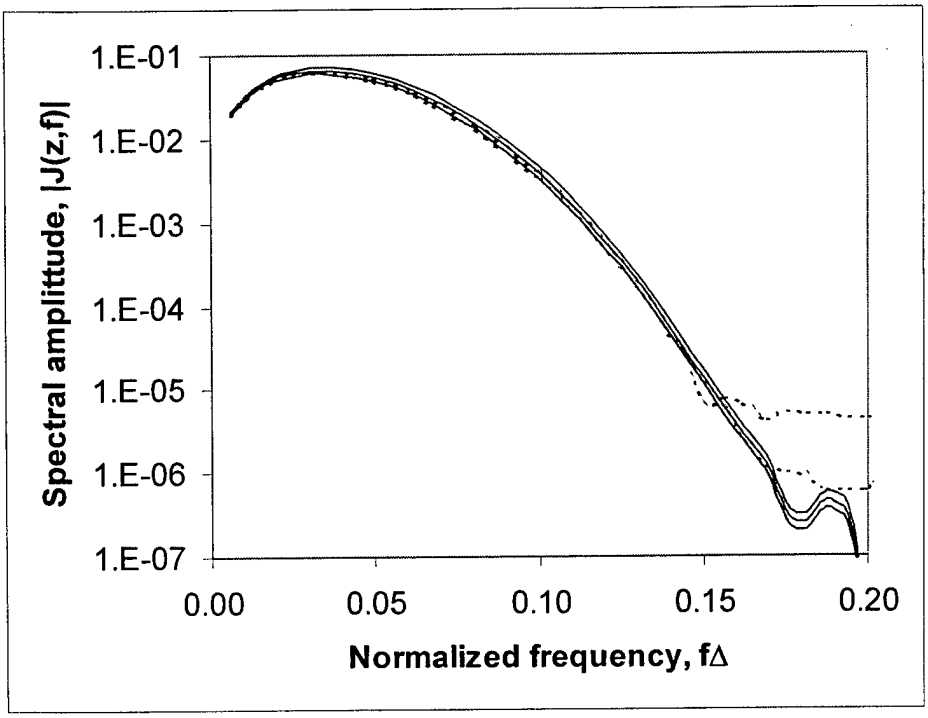

Figure 6-4. Frequency spectra of a bipolar pulse propagated in a lossy transmission line at locations z = 0, 40 cΔ, & 80 cΔ; solid line is analytic and dashed line is efficient MFIE.

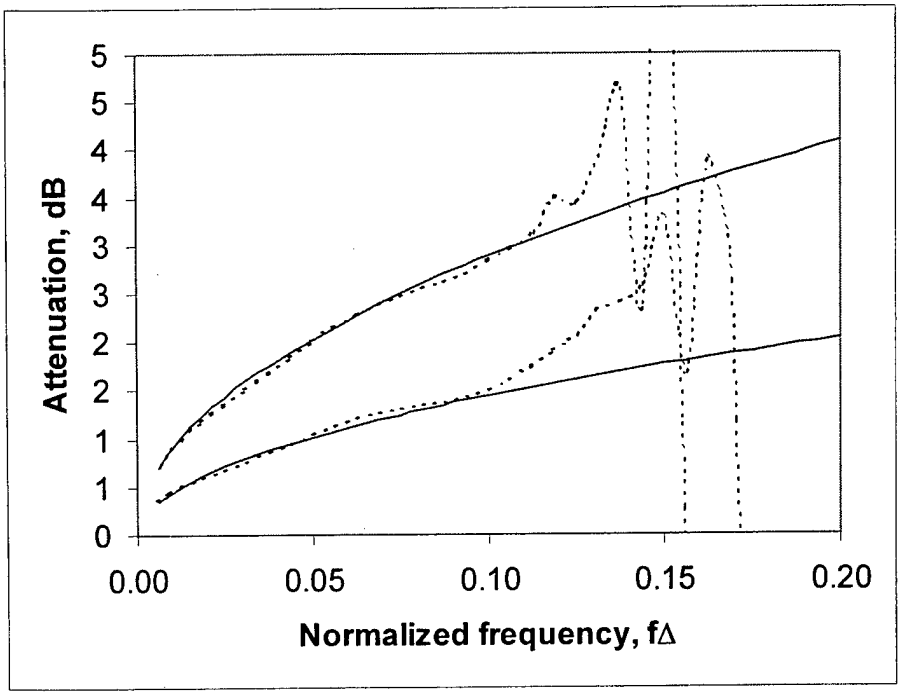

Figure 6-5. Attenuation of a bipolar pulse propagated in a lossy transmission line at locations z = 0, 40 cΔ, & 80 cΔ; solid line is analytic and dashed line is efficient MFIE.

SECTION 7

COMPUTATIONAL CODES

Several computational codes have been developed during the present effort. They are all written in Interactive Data Language (IDL), a product of Research Systems Inc. in Boulder, CO. These codes were written for research purposes only, and are not intended to be user-friendly tools.

LOSSYLINE is a main program that calculates the efficient solution of the dispersive time-domain integral equation for a lossy 2D planar transmission line.

```
; main program lossyline
n=160
a=5.
gw=8.
pi=double(4.*atan(1.))
self=double(alog(2.+sqrt(3.))/pi+1./3.)
beta=double(1000.); =timestep*sigma/epsilon/2
con0=double(1./sqrt(2.*pi*beta))
c=[1.2024728d0,2.5876867d-1,5.6953491d-2,1.2455136d-2,2.7406290d-3, $
5.9659851d-4,1.3367602d-4,2.6443598d-5,8.4750592d-6,9.2249234d-7]
w=[3.d0,1.0908399d0,3.9664388d-1,1.4422497d-1,5.2442115d-2, $
1.9068649d-2,6.9336146d-3,2.5211542d-3,9.1672520d-4,3.3333345d-4]
mm=n_elements(w)
cow=c/w/sqrt(beta)
expw=exp(-w)
jj=dblarr(n,n)
con=dblarr(n,n)
conm=dblarr(n,n,mm)
incident,n,a,jj,gw
for t=1,n-1 do begin
print,t
 for z=1,t-1 do begin
 if (t gt 1) then for m=0,mm-1 do conm(z,t,m)=conm(z,t-1,m)*expw(m) $
 +cow(m)*expw(m)*(1.-expw(m))*jj(z,t-1)
 con(z,t)=total(float(conm(z,t,*)))
 jj(z,t)=(jj(z,t)+uzint(n,jj,a,z,t,con,con0)+uzint(n,jj,0.,z,t,con,con0) $
 +(jj(z,t-1)*con0-(con(z,t)-con(z,t-1)))*self)/(1.+con0*self)
 endfor ; z
endfor ; t
ymin=-1
plot,jj(0,*),yrange=[ymin,1],title='propagated wave vs time'
for z=10,n-1,10 do oplot, jj(z,*)
oplot,[0,n-1],[1,1]
```

```
end
```

INCIDENT is a subroutine that calculates an incident waveform for either the LOSSYLINE or IDEALLINE.

```
pro incident,n,a,jj,gw
t=double(findgen(n))
pi=double(4.*atan(1.))
j0=double(exp(-(t/gw-2.5)^2)*(1.+cos(pi*(t/2.5/gw-1.))))
j0=j0*double(sin(-pi/2.*(t/2.5/gw-1.)))
j0(0)=0.
j0(5*fix(gw):*)=0.
j0=2.*j0/max(j0)
asq=a*a
for z=0,n-1 do begin
zsq=float(z)^2
za1=fix(sqrt(zsq+asq))+1
for t=z,n-1 do jj(z,t)=.5*h(t-z)
 for t=za1,n-1 do begin
 dum=double(0.)
  for u1=za1,t do begin
  usq=float(u1)^2
  y1=usq-zsq
  if (u1 eq za1) then y0=asq else y0=(u1-1.)^2-zsq
  arg1=double((zsq-asq-2.*zsq*asq/y1)/(zsq+asq))
  arg0=double((zsq-asq-2.*zsq*asq/y0)/(zsq+asq))
  dum=dum+double(.5*((1.-u1)*j0(t-u1)+u1*j0(t-u1+1))*(asin(arg1)-asin(arg0)) $
  +z*(j0(t-u1)-j0(t-u1+1))*(atan(sqrt(y1/asq-1.))-atan(sqrt(y0/asq-1.))))
  endfor ; u1
 jj(z,t)=jj(z,t)-dum/pi
 endfor ; t
endfor ; z
return
end
```

UZINT is a function that calculates the dz' du' integral for LOSSYLINE.

```
function uzint,n,jj,a,z,t,con,con0
zzmax=fix((float(t)^2-float(z)^2-a^2)/2./(t-z))
zzmin=(-fix((float(t)^2-float(z)^2-a^2)/2./(t+z)))
dum1=0.
for zz=zzmin,zzmax do begin
zzz=abs(zz)
alpha=double(sqrt(a^2+float(zz-z)^2))
dum=0.
c1=0.
```

```
d1=0.
for u0=fix(alpha),t-1 do begin
u1=float(u0)+1.
c0=c1
d0=d1
c1=double(sqrt(u1^2-alpha^2))
if (alpha le 0.) then d1=0. else $
d1=double(alog(u1/alpha+sqrt((u1/alpha)^2-1.))) ; asech(alpha/u1)
tau=t-u0
jjj=jj(zzz,*)
;  lossy convolution contribution
if (u0 ge 1) then dum=dum- $
(((jjj(tau)-jjj(tau-1))*con0-(con(zzz,tau)-con(zzz,tau-1)))*(d1-d0))
;  non-lossy contribution
if (a ge 1.) then dum=dum+double(a*(jjj(tau)-jjj(tau-1))*(c1-c0)/alpha^2)
endfor ; u
dum1=dum1+dum*(fix(zz gt 0)-fix(zz lt 0))
endfor ; zz
return, dum1/double(4.*atan(1.))
end
```

IDEALLINE is a main program that calculates a a time-domain integral equation solution for the ideal 2D planar transmission line.

```
; main program idealline
n=160
gw=8.
a=2.
jj=fltarr(n,n)
incident,n,a,jj,gw
for t=1,n-1 do begin
print,t
for z=1,t-1 do jj(z,t)=jj(z,t)+uzinti(n,jj,a,z,t)
endfor ; t
ymin=0
plot,jj(*,0),yrange=[ymin,1],title='propagated wave vs distance'
for t=10,n-1,10 do oplot,jj(*,t)
oplot,[0,n-1],[1,1]
plot,jj(0,*),yrange=[ymin,1],title='propagated wave vs time'
for z=10,n-1,10 do oplot, jj(z,*)
oplot,[0,n-1],[1,1]
end
```

UZINTI is a function that returns the dz' du' integral for LOSSYLINE.

```
function uzinti,n,jj,a,z,t
zzmax=fix((float(t)^2-float(z)^2-a^2)/2./(t-z))
zzmin=(-fix((float(t)^2-float(z)^2-a^2)/2./(t+z)))
dum1=0.
for zz=zzmin,zzmax do begin
zzz=abs(zz)
alpha=sqrt(a^2+float(zz-z)^2)
dum=0.
c1=0.
for u0=fix(alpha),t-1 do begin
u1=float(u0)+1.
c0=c1
c1=sqrt(u1^2-alpha^2)
tau=t-u0
jjj=jj(zzz,*)
dum=dum+a*(jjj(tau)-jjj(tau-1))*(c1-c0)/alpha^2
endfor ; u0
dum1=dum1+dum*(fix(zz gt 0)-fix(zz lt 0))
endfor ; zz
return, dum1/(4.*atan(1.))
end
```

ANALYTIC is a main program that compares the analytic and computational solutions. It runs immediately after LOSSYLINE and assumes that the variables jj and beta area available.

```
; main program analytic
pi=4.*atan(1.)
dt=1.
t=dt*findgen(n)
freq=indgen(n)
n21=n/2+1
freq(n21)=n21-n+findgen(n21-2)
freq=freq/float(n)/dt
w=2.*pi*freq
f=freq(0:n/2)
i=complex(0.,1.)
k=w ; wavenumber for speed of light =1.
u=[0.,sqrt(2.*abs(w(1:*))/(2.*beta))/a/abs(k(1:*))]
aa=sqrt(sqrt(1.+2.*u+2.*u^2)+1+u)
gamma=sqrt(abs(w)/(2.*beta))/a/aa+i*k*aa/sqrt(2.)
j0=jj(0,*)
spec0=fft(j0,-1)
spec40a=spec0*exp(-40.*gamma)
spec80a=spec0*exp(-80.*gamma)
spec120a=spec0*exp(-120.*gamma)
```

```
j40a=float(fft(spec40a,1))
j80a=float(fft(spec80a,1))
j120a=float(fft(spec120a,1))
spec40c=fft(jj(40,*),-1)
spec80c=fft(jj(80,*),-1)
plot_io,f,abs(spec0),xrange=[0,.20],yrange=[1e-7,.1],yticks=6, $
title='abs(spectrum) vs frequency'
oplot,f,abs(spec40a)
oplot,f,abs(spec80a)
oplot,f,abs(spec40c),linestyle=9
oplot,f,abs(spec80c),linestyle=9
plot,t,j0,xrange=[0,160.],xticks=8,yrange=[-1,1],$
title='Propagated wave vs time at z=0,40,80,120'
oplot,t,j40a
oplot,t,j80a
oplot,t,j120a
oplot,t,jj(40,*),linestyle=9
oplot,t,jj(80,*),linestyle=9
oplot,t,jj(120,*),linestyle=9
db=20./alog(10.)
plot,f,db*80.*float(gamma),xrange=[0,.2], $
title='Attenuation (dB) vs frequency at z=40,80'
oplot,f,db*40.*float(gamma)
oplot,f,db*alog(abs(spec0/spec40c)),linestyle=9
oplot,f,db*alog(abs(spec0/spec80c)),linestyle=9
end
```

EXPFIT is a main program that fits Z_1 with a sum of exponentials.

```
; main program expfit
pi=4.*atan(1.)
n=100
m=10
q=3.
tmax=1.e3
tmin=1.
time=tmin*exp(alog(tmax/tmin)*findgen(n)/float(n-1))
zz=1./sqrt(pi*(2.*time)^3) ;*(1.+3./8/time+45./128./time^2+525./1024./time^3)
w=double(q/tmin*exp(-findgen(m)*alog(tmax/tmin*q^2)/float(m-1)))
expw=exp(-w)
a=dblarr(m,m)
b=dblarr(m)
f=dblarr(m,n)
for i=0,m-1 do begin
for k=0,n-1 do f(i,k)=exp(-w(i)*time(k))/zz(k)
```

```
b(i)=total(f(i,*))
endfor
for i=0,m-1 do begin
for j=0,m-1 do a(i,j)=total(f(i,*)*f(j,*))
endfor
bb=max(b)
c=cramer(a/bb,b/bb,/double) ; an IDL library routine to solve linear equations
for i=0,m-1 do print,i,c(i),w(i),1./w(i)
print,total(c),total(c*w),total(c/w)
z=dblarr(n)
for k=0,n-1 do z(k)=total(c(*)*exp(-w(*)*time(k)))
plot_oo,time,zz,title='Impedance Z1 vs time: exact and fit'
oplot, time, z, linestyle=9
plot_oi,time,z/zz,yrange=[.99,1.01],title='(exp fit)/exact relative error vs time'
oplot,[tmin,tmax],[1,1]
print,max(zz/z),min(zz/z)
end
```

SECTION 8

REFERENCES

1. P. Drude, *Ann. Physik*, v. 1, p. 566; v. 3, p 869 (1900)

2. J. Bardeen, Electrical conductivity of metals, *J. Appl. Phys.* v. 11, p. 88 (1940)

3. C. Kittel, *Introduction to Solid State Physics*, ch. 7 & 8, Wiley (1971)

4. J. A. Stratton, *Electromagnetic Theory*, ch. 5, McGraw-Hill (1941)

5. L. Bennet and W. L. Weeks, Transient scattering from conducting cylinders, *IEEE Trans. Antennas Propagat.* v. 18, p. 627 (1970)

6. L. Bennet and G. F. Ross, Time-domain electromagnetics and its applications, *Proc. IEEE* v. 66, p. 299 (1968)

7. J. Poggio and E. K. Miller, Integral equation solutions of three-dimensional scattering problems, in *Computer Techniques for Electromagnetics*, ch. 4, R. Mittra ed., Pergamon (1973), Hemisphere (1987)

8. R. Mittra, Integral equation methods for transient scattering, in *Transient Electromagnetic Fields*, ch. 2, L. B. Felsen ed., Springer-Verlag (1976)

9. E. K. Miller, A selective survey of computational electromagnetics, *IEEE Trans. Antennas Propagat.* v. 6, p. 1281 (1988)

10. F. M. Tesche, On the inclusion of loss in time-domain electromagnetic interaction problems, *IEEE Trans. Antennas Propagat.* v. 32, p. 1 (1990)

11. M. J. Bluck, S. P. Walker, & M. D. Pocock, The extension of time-domain integral analysis to scatter from imperfectly conducting bodies, *IEEE Trans. Antennas Propagat.* v. 49, p. 875 (2001)

12. P. M. Morse & H. Feshbach, *Methods of Theoretical Physics*, ch. 7, McGraw-Hill (1953)

13. M. A. Leontovich, *Investigations of Propagation of Radiowaves*, Part II, Academy of Sciences, Moscow (1948)

14. T. B. A. Senior, Impedance boundary conditions for imperfectly conducting surfaces, *Appl. Sci. Res.* v. 8B, p.418 (1960)

15. K. M. Mitzner, An integral equation approach to scattering from a body of finite conductivity, *Radio Science* v. 2, p. 1459 (1967)

16. R. J. Luebbers, F. P. Hunsberger, K. S. Kunz, R. B. Standler, & M. Schneider, A frequency dependent finite difference time domain formulation for dispersive materials, *IEEE Trans. Electromagn Compat.* v. 32, p. 22 (1990)

17. J. S. Maloney & G. S. Smith, The use of surface impedance concepts in the finite-difference time-domain method, *IEEE Trans. Antennas Propagat.* v. 40, p. 38 (1992)

18. K. S. Oh & J. E. Schutt-Aine, An efficient implementation of surface impedance boundary conditions for the finite-difference time-domain method, *IEEE Trans. Antennas Propagat.* v. 43, p. 660 (1995)

19. S. Gradshteyn & I. M. Ryzhik, Table of Integrals, Series, and Products, Academic (1980)

20. S. Ramo, J. R. Whinnery, & T. van Duzer, *Fields and Waves in Communication Electronics*, ch. 7, Wiley (1965)